

# $^{234}\text{Th}$ scavenging and its relationship to acid polysaccharide abundance in the Gulf of Mexico

Laodong Guo<sup>a,\*</sup>, Chin-Chang Hung<sup>b</sup>, Peter H. Santschi<sup>b</sup>, Ian D. Walsh<sup>c</sup>

<sup>a</sup>International Arctic Research Center, University of Alaska Fairbanks, Fairbanks, AK 99775, USA

<sup>b</sup>Department of Oceanography, Texas A&M University, Galveston, TX 77551, USA

<sup>c</sup>College of Oceanic and Atmospheric Sciences, Oregon State University, Corvallis, OR 97331, USA

Received 6 September 2001; received in revised form 31 January 2002; accepted 18 February 2002

## Abstract

Size-fractionated particulate  $^{234}\text{Th}$  and acid polysaccharides (APS) were collected from stations along a transect in the Gulf of Mexico, in order to examine the role of APS content in controlling the extent and rates of  $^{234}\text{Th}$  scavenging in the ocean and to explore, for the first time, the relationship between Th scavenging and biochemical composition of particulate matter. Oceanographically consistent vertical profiles of dissolved and particulate  $^{234}\text{Th}$  concentrations were observed, with a considerable  $^{234}\text{Th}$  deficit relative to  $^{238}\text{U}$  in the upper water column and in benthic nepheloid layers, but reaching secular equilibria between  $^{234}\text{Th}$  and  $^{238}\text{U}$  in intermediate waters. Within the total particulate  $^{234}\text{Th}$  pool ( $>0.5\ \mu\text{m}$ ), the  $10\text{--}53\ \mu\text{m}$  fraction had the largest share of  $^{234}\text{Th}$  (37–57%), followed by the  $>53\ \mu\text{m}$  (13–36%), the  $1\text{--}10\ \mu\text{m}$  (10–21%), and the  $0.5\text{--}1\ \mu\text{m}$  (8–17%) fractions, resulting in a decrease of  $\text{POC}/^{234}\text{Th}$  ratios with increasing particle size. Residence times of  $^{234}\text{Th}$  in size-fractionated particles, calculated with a serial multi-box model, were, as expected, consistently shorter than those for total particulate  $^{234}\text{Th}$ , with the shortest residence times ( $<0.5$  day at coastal stations and  $<1\text{--}5$  days at deep stations) observed in the smaller particulate fractions ( $0.5\text{--}10\ \mu\text{m}$ ), and the large particles  $>53\ \mu\text{m}$ . These results suggest that submicron and micron-sized particles are the most important intermediary in the Th scavenging and that  $^{234}\text{Th}$  on smaller particles ( $<10\ \mu\text{m}$ ) can coagulate into the  $10\text{--}53\ \mu\text{m}$  particles very rapidly, within a time scale of  $<1$  day. A positive correlation between  $^{234}\text{Th}/\text{POC}$  and OC-normalized total APS content was observed, suggesting that exopolymeric fibrillar APS, the surface active substances in seawater, are the most effective organic compounds for Th(IV) scavenging. Most importantly, residence times of particles in the size ranges of  $1\text{--}10$  and the  $>53\ \mu\text{m}$  were also significantly and inversely correlated with uronic acid (URA, a fraction of total APS) concentrations, indicating that the APS content controls not only rates and amounts of  $^{234}\text{Th}$  sorption, but also rates of coagulation of particles. Thus, the biochemical composition of marine particles needs to be considered in improved Th(IV) scavenging models. © 2002 Elsevier Science B.V. All rights reserved.

**Keywords:**  $^{234}\text{Th}$  scavenging; Acid polysaccharide; Size-fractionated particulate; POC;  $^{234}\text{Th}/^{238}\text{U}$

## 1. Introduction

Thorium(IV) is a highly particle reactive element and has strong affinities to particles, especially organic matter in seawater. Among the naturally

\* Corresponding author. Tel.: +1-907-474-2794; fax: +1-907-474-2679.

E-mail address: guol@iarc.uaf.edu (L. Guo).

occurring Th isotopes,  $^{234}\text{Th}$ , with a half life of 24.1 days, has been widely used to trace upper ocean particle dynamics and fluxes of particulate organic matter out of the euphotic zone through the use of  $^{234}\text{Th}/\text{OC}$  and  $^{234}\text{Th}/^{238}\text{U}$  ratios (e.g., Bruland and Coale, 1986; Murray et al., 1989; Cochran et al., 1992; Buesseler et al., 1992a, 1995; Santschi et al., 1999). In addition,  $^{234}\text{Th}$  has also been used as a tracer to examine the residence times of colloidal macromolecular organic matter in the ocean (e.g., Baskaran et al., 1992; Moran and Buesseler, 1993; Huh and Prahl, 1995; Santschi et al., 1995; Guo et al., 1997). Despite the wide applications of Th isotopes in marine organic carbon cycling studies, the detailed molecular mechanisms and the interactions of Th isotopes with different organic matter phases, in particular biomolecules, are still not well understood (Santschi and Honeyman, 1991; Guo et al., 1997). Whether Th(IV) tracks the bulk marine organic matter or preferentially interacts with certain organic compounds, as was recently suggested by Quigley et al. (2002), is of paramount importance when using thorium isotopes as a tracer in marine organic carbon cycling studies.

Recent studies have shown that ratios of  $^{234}\text{Th}/\text{OC}$  could vary with study area, water depth, and particle size fractions in the ocean (e.g., Cochran et al., 1995; Buesseler, 1998 and references therein; Santschi et al., 1999; Burd et al., 2000). The increase of  $^{234}\text{Th}/\text{OC}$  ratios with increasing particle size appears to be inconsistent with the sorption and sinking pathways in the Th(IV) scavenging model, since smaller particles have larger specific surface areas and should have higher  $^{234}\text{Th}/\text{OC}$  ratios, if non-specific and non-selective sorption reactions are controlling  $^{234}\text{Th}$  uptake (Quigley et al., 1996). Therefore, differences in  $^{234}\text{Th}/\text{OC}$  ratios imply that the interactions of Th isotopes with marine organic matter could be highly selective and chemical composition related, or that other processes, such as bacterial and zooplankton activities and coagulation of surface-active ligands, are coupled to the sorption reaction. Indeed,  $^{234}\text{Th}$  studies have been interpreted by assuming that transparent exopolymeric particles (TEP) could play an important role in the  $^{234}\text{Th}$  scavenging (e.g., Niven et al., 1997). However, acid polysaccharide (APS) containing TEP particles had not been measured, and there are no studies that tested this assumption in the field. Most recently, Quigley et al. (2002) tested this

assumption in controlled laboratory experiments, and the results revealed that most of the Th(IV) is tightly bound to surface-active APS biopolymers, which rapidly coagulate into larger particles (Quigley et al., 2002). Since this conclusion, derived from controlled laboratory experiments, may not necessarily be applicable to field situations, oceanic observations on  $^{234}\text{Th}$ –APS relationships are therefore indispensable. In addition, to better use Th isotopes as tracers for POC fluxes and organic carbon cycling, our knowledge regarding the distribution and partitioning of Th isotopes among dissolved and particulate phases, and the relationship between Th(IV) uptake and chemical composition of particles in the ocean, needs to be improved.

In the present study, the scavenging of  $^{234}\text{Th}$  and its phase partitioning among different size fractions, namely, the <0.5, 0.5–1, 1–10, 10–53, and >53  $\mu\text{m}$ , were examined in contrasting oceanographic settings, a cold-core ring (CCR) vs. a warm-core ring (WCR), in the Gulf of Mexico. At the same time, the partitioning of total acid polysaccharides (APS), total carbohydrate (CHO), and total uronic acids (URA, a fraction of total APS) among different particle sizes was also investigated. This allowed us, for the first time, to derive relationships between the size-fractionated  $^{234}\text{Th}$  and total APS content, as well as between  $^{234}\text{Th}$ -derived residence times and APS content, using a serially linked multi-box model approach.

## 2. Materials and methods

### 2.1. Study area

Seawater samples were collected for measurements of  $^{234}\text{Th}$  and polysaccharides in the Gulf of Mexico during July 1–10, 2000, aboard the R/V Gyre. Sampling stations were designed to cover different oceanographic settings, including a cold-core ring (CCR) and a warm core ring (WCR), along a transect at  $\sim 95^\circ\text{W}$  in the northwest Gulf of Mexico. Details of the sampling locations and ancillary data for surface waters are listed in Table 1. Note that station 5 with a surface water temperature of  $28.81^\circ\text{C}$ , was located within a CCR, whereas station 7 was a WCR, with a surface water temperature of  $29.40^\circ\text{C}$ . As shown in Table 1, surface water salinity increased from station 1

Table 1  
Sampling locations and surface water ancillary data

Station	Location	Water depth (m)	Surface water salinity	Temperature (°C)	Chl- <i>a</i> (µg/l)
1	28 51N; 94 19W	25	35.289	28.85	0.202
2	28 50N; 94 59W	20	35.400	29.69	0.194
3	28 28N; 95 25W	25	35.751	29.42	0.180
4	28 00N; 95 26W	75	36.100	28.87	0.174
5	27 30N; 95 11W	985	36.322	28.81	0.087
6	26 55N; 95 16W	1500	36.556	28.89	0.071
7	26 00N; 95 20W	1600	36.680	29.40	0.042

to station 7, while surface water Chl-*a* concentrations decreased consistently from station 1 to station 7.

## 2.2. Filter impregnation procedures

Dissolved  $^{234}\text{Th}$  was extracted from seawater on  $\text{MnO}_2$  impregnated polypropylene fiber cartridges (Baskaran et al., 1993). The  $\text{MnO}_2$  impregnated filters were manufactured using the following procedure. First, the filters were rinsed for 5 to 10 min using filtered tap water (through a series of filters including two  $\text{MnO}_2$  impregnated filters) and soaked overnight in a 0.5- to 1-M NaOH solution heated at  $\sim 60^\circ\text{C}$ . Then, filters were soaked in a heated 3 M HCl solution overnight. Between chemical solutions, filters were rinsed with filtered tap water for 10 to 20 min to remove any residual chemicals. Finally, the cleaned filters were introduced into a heated ( $60\text{--}80^\circ\text{C}$ ) 0.4 M  $\text{KMnO}_4$  solution for 8–10 h. After a final rinse, each filter was bagged wet and dated. Laboratory spike  $^{234}\text{Th}$  experiments were carried out to ensure high extraction efficiency and quality of impregnated  $\text{MnO}_2$  filters (Santschi et al., 1999).

## 2.3. Sampling of dissolved and size fractionated particulate $^{234}\text{Th}$

Dissolved and size fractionated particulate  $^{234}\text{Th}$  were extracted from seawater using either a submersible pump for the upper water column (shallower than 120 m) or a multiple in situ pumping system (MIPS) for deep waters (Baskaran et al., 1993; Guo et al., 1995; Santschi et al., 1999). Both submersible pump and MIPS were equipped with a series of six filters (polypropylene, Sparkling Clear Industries),

with nominal pore sizes of 53, 10, 1, 0.5  $\mu\text{m}$ , followed by two  $\text{MnO}_2$ -impregnated 0.5  $\mu\text{m}$  pore-sized filters. The first four consecutive filters were designed to collect  $^{234}\text{Th}$  in size-fractionated particulate phases ( $>0.5\ \mu\text{m}$ ), while the last two  $\text{MnO}_2$ -impregnated filters were intended to extract the  $<0.5\ \mu\text{m}$  dissolved  $^{234}\text{Th}$ , with the last filter used for the extraction efficiency correction (Buesseler et al., 1992b; Cochran et al., 1995). Therefore, the six filters resulted in five different size fractions of  $^{234}\text{Th}$ , namely the  $>53$ , 10–53, 1–10, 0.5–1, and  $<0.5\ \mu\text{m}$ . Large volumes of seawater (up to 1000–4000 l) were used to ensure that all size-fractionated particulate  $^{234}\text{Th}$  fractions had sufficiently high activity and precision.

After a predetermined amount of water was pumped through the filters, the volume and pumping time were recorded. Similar flow rates were held for most samples, but in some cases were varied in order to examine the relationship between  $^{234}\text{Th}$  extraction efficiency and pumping flow rate (see next section). When pumping was completed, filters were removed, labeled and placed in individual ziplock bags to be analyzed for  $^{234}\text{Th}$  in the laboratory.

## 2.4. Determination of $^{234}\text{Th}$

Filter samples, including two Mn-impregnated filters and four different pore-sized filters, were combusted at  $550^\circ\text{C}$  for 4 h. After cool-down, the samples were then individually packed into counting vials to result in weight to volume ratios similar to those of standard solutions that were used to calibrate the detector's geometry. The gamma emission of  $^{234}\text{Th}$  was determined at 63 keV on a Canberra ultra

high purity Germanium well detector (Santschi et al., 1999). Counting times were adjusted to result in a propagated error of <2–10% or better, depending on sample sizes. Decay corrections were applied to correct to the mid-time of sampling. Errors reported here are one-sigma standard errors.

### 2.5. $^{234}\text{Th}$ extraction efficiency

The extraction efficiency, Eff, was calculated using the following relationship:

$$\text{Eff} = 1 - \frac{[^{234}\text{Th}]_B}{[^{234}\text{Th}]_A} \quad (1)$$

where  $[^{234}\text{Th}]_A$  is the  $^{234}\text{Th}$  activity of the first filter, filter A, and  $[^{234}\text{Th}]_B$  is the  $^{234}\text{Th}$  activity of the second filter, filter B (e.g., Buesseler et al., 1992b; Baskaran et al., 1993; Cochran et al., 1995). The extraction efficiency, tested under laboratory conditions using coastal seawater and low pumping rates ( $\sim 10$  l/min), was high, ranging from 93.6% to 96.7%. However, field samples using higher pumping speeds (or flow rates) resulted in lower extraction efficiencies, varying from 70% to 92%. Extraction efficiency decreases with increasing flow rates, especially for deep-water samples, which had a relatively high and constant dissolved  $^{234}\text{Th}$  activity. The relationship between extraction efficiency (Eff) and flow rate (FR, l/min) can be described as:

$$\text{Eff} = 0.898 - 0.00277 \times \text{FR} \quad (R = 0.762) \quad (2)$$

with  $p < 0.005$ . However, this relationship for surface water samples is somewhat weaker. Our results on the decreased extraction efficiency with increasing flow rate are consistent with those reported previously (e.g., Cochran et al., 1995; Charette and Moran, 1999). In addition, our consistently high efficiency values (with an average of  $0.84 \pm 0.07$ ) indicate that all experimental procedures, including Mn-impregnated filter preparation, sample processing, and gamma counting were optimal, which ensured that  $^{234}\text{Th}$  data presented here are reliable. Excellent duplicate results of a surface water sample at 2 m from station 5 further confirmed the precision of our  $^{234}\text{Th}$  data (Table 2).

### 2.6. Measurements of polysaccharides in different particle size fractions

The different size fractionated particles (0.7–10, 10–53, and  $>53$   $\mu\text{m}$ ) were also collected for organic carbon and polysaccharide determinations (Hung et al., submitted for publication). After samples were dried, filters were cut and weighed for OC measurements after removing inorganic carbon by HCl acid fume (Hedges and Stern, 1984) and for determinations of polysaccharide fractions, i.e., total APS, uronic acids (a fraction of total APS), and total carbohydrates (Hung et al., 2001). Organic carbon was quantified on a CHNS/O elemental analyzer (Guo and Santschi, 1997). Detailed procedures for total polysaccharides and uronic acids are described in Hung and Santschi (2000) and Hung et al. (2001), while those of total APS are presented in Hung et al. (submitted for publication).

Briefly, the concentration of APS in the particulate phase was measured by an alcian blue stain method (Passow et al., 1994), using extensive re-calibrations and other modifications (Hung et al., submitted for publication). Particles were stained by alcian blue for 2 s and washed with  $\text{d-H}_2\text{O}$  to remove the excess alcian blue dye. The stained particles were dissolved in 4 ml of 80% sulfuric acid for 2 h and centrifuged at 1000 rpm for 5 min. Finally, the absorbance of the supernatant solution was measured at 787 nm in a 1-cm cuvette. Standard curves with different APS standard compounds were determined after correction for the actual amount of standard CHO (rather than artifact-prone filter net weight increase), which was retained by the filter. The concentration of APS was expressed as  $\mu\text{M-C}$  alginic acid equivalents, as alginic acids are major classes of APS.

Conditions, under which results reported as  $\mu\text{M-C}$  alginic acid equivalents can be considered in a quantitative way, require that sulfated polysaccharides make up only a minor fraction of APS, as carrageenan standard curves were different from those of alginic acid. Since producers of sulfated polysaccharides, such as macroalgae (e.g., *Sargassum n.* or *Chondrus crispus*), present only in surface waters, and diatoms, which were present in the water column at low abundance (i.e., less than 10% of Chl-*a* equivalents), and because sulfated APS are only a minor component in total APS excreted by Prochlor-

Table 2

Water depth, salinity, and activity concentrations of  $^{238}\text{U}$ , dissolved, particulate, total  $^{234}\text{Th}$ , and size fractionated particulate  $^{234}\text{Th}$  (dpm/l)

Station	Depth (m)	Salinity	$^{238}\text{U}$ (dpm/l)	Dissolved (<0.5 $\mu\text{m}$ )	Particulate (>0.5 $\mu\text{m}$ )	Total $^{234}\text{Th}$ (dpm/l)	$^{234}\text{Th}/^{238}\text{U}$ Ratio	0.5–1 $\mu\text{m}$ particulate	1–10 $\mu\text{m}$ particulate	10–53 $\mu\text{m}$ particulate	>53 $\mu\text{m}$ particulate
1	2	35.289	2.499	0.708 ± 0.010	0.087 ± 0.015	0.795 ± 0.018	0.318	0.0073 ± 0.0005	0.0119 ± 0.0009	0.0585 ± 0.0028	0.0096 ± 0.0007
2	2	35.400	2.507	0.367 ± 0.010	0.127 ± 0.015	0.494 ± 0.018	0.197	0.0121 ± 0.0011	0.0381 ± 0.0021	0.0408 ± 0.0019	0.0362 ± 0.0022
3	2	35.751	2.532	0.493 ± 0.007	0.135 ± 0.011	0.628 ± 0.013	0.248	0.0121 ± 0.0006	0.0305 ± 0.0020	0.0584 ± 0.0039	0.0343 ± 0.0019
3	22	35.751	2.532	0.261 ± 0.006	0.141 ± 0.013	0.403 ± 0.014	0.159	0.0087 ± 0.0006	0.0223 ± 0.0014	0.0958 ± 0.0096	0.0148 ± 0.0009
4	2	36.100	2.556	0.932 ± 0.015	0.131 ± 0.022	1.063 ± 0.027	0.416	0.0144 ± 0.0005	0.0115 ± 0.0005	0.0710 ± 0.0036	0.0341 ± 0.0017
4	50	36.100	2.556	0.876 ± 0.023	0.216 ± 0.034	1.092 ± 0.042	0.427	0.0092 ± 0.0006	0.0354 ± 0.0023	0.0934 ± 0.0063	0.0777 ± 0.0047
5	2	36.322	2.572	1.308 ± 0.026	0.112 ± 0.037	1.420 ± 0.045	0.552	0.0143 ± 0.0008	0.0192 ± 0.0008	0.0612 ± 0.0029	0.0177 ± 0.0011
	2-B	36.322	2.572	1.261 ± 0.025	0.229 ± 0.036	1.489 ± 0.044	0.579	0.0282 ± 0.0017	0.0514 ± 0.0023	0.0875 ± 0.0063	0.0615 ± 0.0030
	10	36.317	2.572	1.371 ± 0.024	0.141 ± 0.034	1.512 ± 0.042	0.588	0.0310 ± 0.0016	0.0340 ± 0.0020	0.0443 ± 0.0036	0.0317 ± 0.0025
	30	36.319	2.572	1.471 ± 0.030	0.142 ± 0.043	1.613 ± 0.052	0.627	0.0149 ± 0.0009	0.0477 ± 0.0034	0.0562 ± 0.0027	0.0237 ± 0.0017
	65	36.409	2.578	1.620 ± 0.024	0.116 ± 0.034	1.736 ± 0.042	0.673	0.0174 ± 0.0011	0.0324 ± 0.0025	0.0476 ± 0.0025	0.0184 ± 0.0012
	75	36.414	2.579	1.568 ± 0.020	0.105 ± 0.028	1.674 ± 0.034	0.649	0.0117 ± 0.0008	0.0190 ± 0.0010	0.0606 ± 0.0046	0.0139 ± 0.0011
	300	36.387	2.577	1.800 ± 0.038	0.449 ± 0.056	2.247 ± 0.068	0.872	0.0365 ± 0.0010	0.0840 ± 0.0070	0.0660 ± 0.0041	0.2622 ± 0.0101
	800	35.832	2.537	2.190 ± 0.021	0.319 ± 0.032	2.506 ± 0.038	0.988	0.0467 ± 0.0015	0.0330 ± 0.0024	0.1548 ± 0.0087	0.0849 ± 0.0052
6	2	36.556	2.589	1.756 ± 0.035	0.157 ± 0.049	1.913 ± 0.060	0.739	0.0248 ± 0.0011	0.0244 ± 0.0017	0.0632 ± 0.0029	0.0445 ± 0.0022
	10	36.605	2.592	2.079 ± 0.039	0.119 ± 0.055	2.199 ± 0.067	0.848	0.0195 ± 0.0012	0.0221 ± 0.0014	0.0574 ± 0.0027	0.0203 ± 0.0011
	30	36.599	2.592	1.790 ± 0.043	0.214 ± 0.061	2.004 ± 0.075	0.773	0.0292 ± 0.0015	0.0557 ± 0.0048	0.0681 ± 0.0037	0.0612 ± 0.0055
	40	36.558	2.589	1.964 ± 0.041	0.195 ± 0.058	2.158 ± 0.071	0.834	0.0306 ± 0.0016	0.0311 ± 0.0023	0.1045 ± 0.0093	0.0284 ± 0.0022
	74	36.451	2.581	2.265 ± 0.039	0.237 ± 0.056	2.502 ± 0.068	0.969	0.0303 ± 0.0015	0.0315 ± 0.0025	0.0879 ± 0.0091	0.0875 ± 0.0075
	120	36.417	2.579	2.221 ± 0.037	0.163 ± 0.011	2.384 ± 0.039	0.924	–	–	–	–
	500	36.417	2.572	2.320 ± 0.037	0.308 ± 0.021	2.624 ± 0.043	1.020	–	–	–	–
	1000	34.920	2.473	2.120 ± 0.026	0.139 ± 0.006	2.257 ± 0.027	0.913	–	–	–	–
	1360	34.971	2.476	2.020 ± 0.041	0.118 ± 0.004	2.141 ± 0.041	0.865	–	–	–	–
7	10	36.672	2.597	1.900 ± 0.031	0.222 ± 0.045	2.122 ± 0.055	0.817	0.0428 ± 0.0021	0.0515 ± 0.0040	0.0976 ± 0.0084	0.0304 ± 0.0020
	35	36.674	2.597	1.942 ± 0.034	0.152 ± 0.048	2.094 ± 0.059	0.806	0.0156 ± 0.0009	0.0320 ± 0.0016	0.0804 ± 0.0040	0.0241 ± 0.0013
	45	36.509	2.585	2.078 ± 0.045	0.180 ± 0.063	2.258 ± 0.077	0.873	0.0094 ± 0.0012	0.0553 ± 0.0034	0.0904 ± 0.0054	0.0248 ± 0.0015
	75	36.512	2.585	1.951 ± 0.033	0.239 ± 0.047	2.190 ± 0.057	0.847	0.0446 ± 0.0023	0.0539 ± 0.0039	0.1069 ± 0.0084	0.0332 ± 0.0017
	121	36.484	2.583	1.820 ± 0.033	0.181 ± 0.046	1.998 ± 0.057	0.773	0.0154 ± 0.0009	0.0270 ± 0.0012	0.0823 ± 0.0022	0.0559 ± 0.0037
	202	36.442	2.581	2.08 ± 0.015	0.253 ± 0.021	2.332 ± 0.026	0.904	0.0278 ± 0.0004	0.0522 ± 0.0016	0.1036 ± 0.0020	0.0690 ± 0.0021
	500	36.754	2.603	2.139 ± 0.046	0.421 ± 0.068	2.559 ± 0.082	0.983	0.0276 ± 0.0015	0.0828 ± 0.0059	0.2358 ± 0.0172	0.0743 ± 0.0047
	1000	34.909	2.472	1.934 ± 0.029	0.274 ± 0.042	2.207 ± 0.051	0.893	0.0576 ± 0.0023	0.0451 ± 0.0032	0.1144 ± 0.0085	0.0566 ± 0.0030
	1500	34.969	2.476	1.784 ± 0.028	0.217 ± 0.041	2.002 ± 0.050	0.808	0.0387 ± 0.0025	0.0463 ± 0.0034	0.0982 ± 0.0079	0.0341 ± 0.0021

ophytes, Cyanobacteria and Haptophytes (e.g., De Philippis and Vincenzini, 1998), the dominant species encountered at that time in the Gulf of Mexico water column, we maintain that our improved APS technique can be used in a quantitative sense. Results on distributions and production of polysaccharides are presented elsewhere (Hung et al., submitted for publication).

### 3. Results and discussion

#### 3.1. Variations of dissolved and particulate $^{234}\text{Th}$ in the water column

Activity concentrations of dissolved, particulate and size-fractionated  $^{234}\text{Th}$  are listed in Table 2. While  $^{238}\text{U}$  concentrations (calculated using the relationship  $^{238}\text{U} \text{ (dpm/l)} = 0.07081 \times \text{salinity}$ , Ku et al., 1977) changed little at all stations and water depths, total  $^{234}\text{Th}$  concentration varied significantly from Sta-1 to Sta-7, ranging from 0.5–0.8 dpm/l at nearshore stations to 1.42–2.56 dpm/l at offshore and open gulf stations. Using the  $^{234}\text{Th}/^{238}\text{U}$  ratio as a scavenging index, Sta-1 to Sta-4 had relatively low  $^{234}\text{Th}/^{238}\text{U}$  ratios, with values  $< 0.42$  (Table 2). Lower  $^{234}\text{Th}/^{238}\text{U}$  ratios and thus more intensive  $^{234}\text{Th}$  scavenging rates are coincident with, and likely related to higher Chl-*a* concentrations at these stations (Table 1). The  $^{234}\text{Th}/^{238}\text{U}$  ratios at Sta-5 (CCR station) were lower than those at Sta-6 and Sta-7, consistent with their higher nutrient, POC and Chl-*a* concentrations due to upwelling at the CCR station.

Vertical profiles of dissolved ( $< 0.5 \mu\text{m}$ ), particulate ( $> 0.5 \mu\text{m}$ ) and total  $^{234}\text{Th}$  activity concentrations, along with  $^{238}\text{U}$  concentration (dpm/l) are shown in Fig. 1. As is evident from these vertical profiles, a significant deficit of total  $^{234}\text{Th}$ , relative to its mother nuclide,  $^{238}\text{U}$ , was observed in the upper water column at all three stations. At Sta-6 and Sta-7, this intensive  $^{234}\text{Th}$  scavenging occurred not only in the upper water column, but also in the bottom waters below 1000 m (Fig. 1).

Station 5 is a CCR station which contains more coastal waters and high Chl-*a* concentrations, and therefore shows the most extensive scavenging of  $^{234}\text{Th}$  (up to 1.0 dpm/l  $^{234}\text{Th}$  deficit) in the upper water column compared to both Sta-6 and Sta-7.

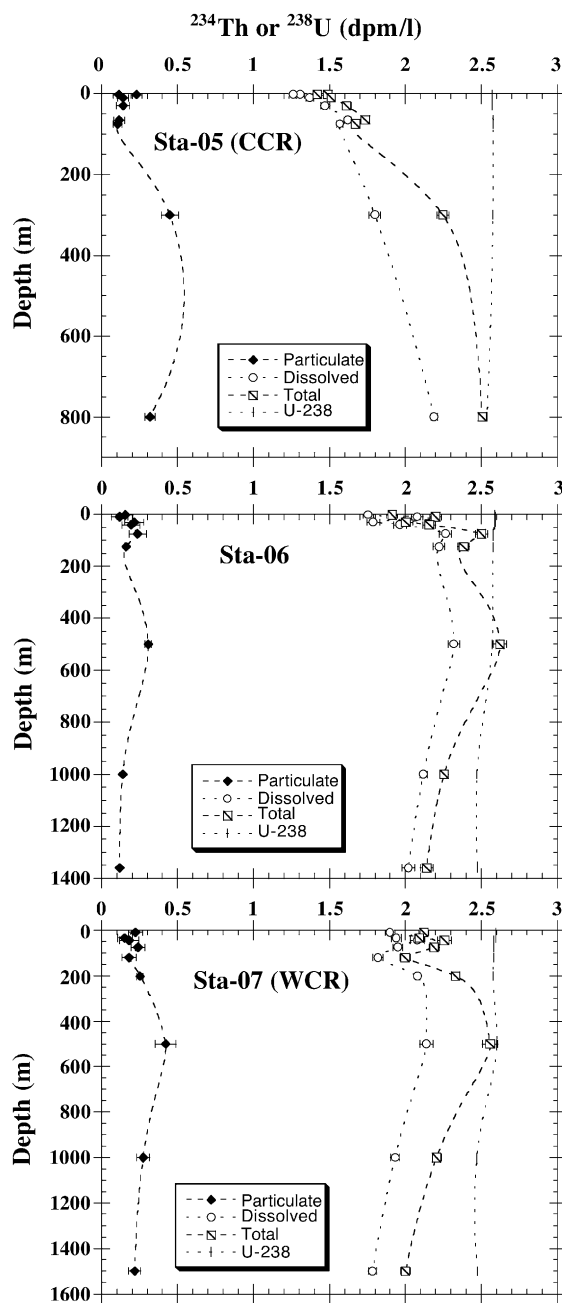


Fig. 1. Vertical distributions of dissolved, particulate, and total  $^{234}\text{Th}$  (dpm/l) and  $^{238}\text{U}$  at stations 5, 6, and 7, showing two distinct regions with  $^{234}\text{Th}$  deficiencies, i.e., the euphotic and benthic boundary layer zone, separated by a secular equilibrium zone between 500 and 800 m water depth. Station 5 was within a cold-core ring and station 7 was within a warm-core station while station 6 was located in the boundary between the CCR and WCR.

Station 7 is a WCR station, which contains mostly oligotrophic Caribbean waters and lower Chl-*a* concentrations (Table 1). Consequently, the total  $^{234}\text{Th}$  deficit at Sta-7 is only  $<0.5$  dpm/l in the upper water column (Fig. 1). While  $^{234}\text{Th}/^{238}\text{U}$  disequilibria existed in the upper water column at all three stations, a  $^{234}\text{Th}$  deficit in bottom waters was not observed at the shallower Sta-5, in contrast to bottom waters at the deeper Sta-6 and Sta-7, where disequilibrium of  $^{234}\text{Th}/^{238}\text{U}$  prevailed. Bottom water  $^{234}\text{Th}/^{238}\text{U}$  disequili-

bria have recently been reported for different oceanic environments (e.g., Bacon and Rutgers van der Loeff, 1989, for the Pacific, Baskaran et al., 1996, for the Gulf of Mexico, Santschi et al., 1999, for the Middle Atlantic Bight, Moran and Smith, 2000, for the Arctic). Significant  $^{234}\text{Th}$  deficiencies in bottom waters at Sta-6 and Sta-7 are likely due to the existence of benthic nepheloid layers, caused by strong bottom currents in the Gulf of Mexico (e.g., Hamilton and Lugo-Fernandez, 2001).

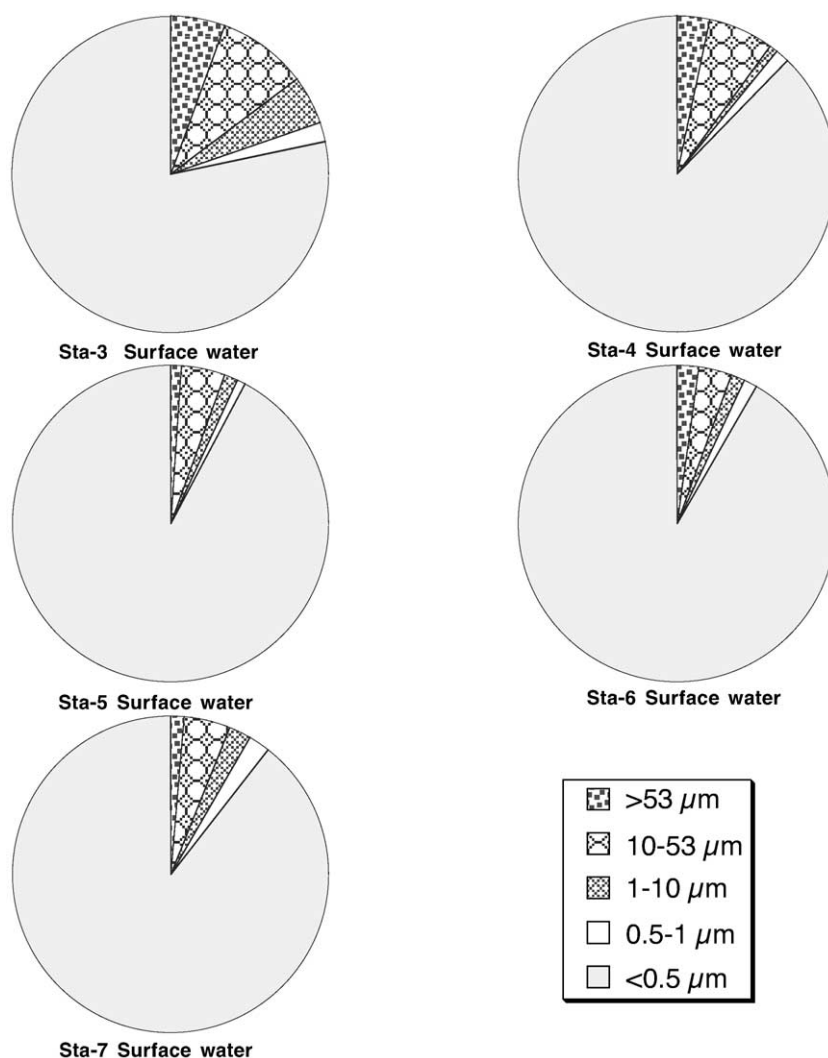


Fig. 2. Partitioning of  $^{234}\text{Th}$  between dissolved and particulate and size-fractionated particles in surface waters at stations in the Gulf of Mexico.

### 3.2. Partitioning of $^{234}\text{Th}$ between dissolved and size-fractionated particulate phases

Activity concentrations of  $^{234}\text{Th}$  in dissolved and particulate phases as well as in size fractionated particulate fractions, are listed in Table 2 and summarized in Figs. 2 and 3. In general, the total particulate  $^{234}\text{Th}$  ( $>0.5\ \mu\text{m}$ ) concentrations decreased from nearshore to offshore stations in both surface and bottom waters. Partitioning of  $^{234}\text{Th}$  between dissolved and particulate phases show that the percentage of the dissolved ( $<0.5\ \mu\text{m}$ )  $^{234}\text{Th}$  in surface waters ranged from 78% to 92%, increasing from nearshore to offshore stations, whereas the particulate ( $>0.5\ \mu\text{m}$ )  $^{234}\text{Th}$  percentage in surface waters varied from 8% to 22%, decreasing from nearshore to offshore stations (Fig. 2). For bottom water samples, the percentage of particulate  $^{234}\text{Th}$  was relatively higher than that of surface waters. For example, the percentage of the dissolved ( $<0.5\ \mu\text{m}$ )  $^{234}\text{Th}$  in bottom waters was only 65% at Sta-3 but 89% at Sta-7 (Fig. 3).

Within the total particulate phase, the 10–53  $\mu\text{m}$  fraction had the highest percentage of  $^{234}\text{Th}$ , followed by the  $>53\ \mu\text{m}$  particulate fraction, and then the 1–10 and the 0.5–1  $\mu\text{m}$  fractions. The last two size fractions thus had the lowest share of the total particulate  $^{234}\text{Th}$  phase. Using available size fractionation POC and  $^{234}\text{Th}$  data (Tables 2 and 3), the  $>53\ \mu\text{m}$  particles had the lowest POC/ $^{234}\text{Th}$  ratio (with an average of 3.1  $\mu\text{mol/dpm}$ ), followed by the 10–53  $\mu\text{m}$  (an average POC/ $^{234}\text{Th}$  of 3.6  $\mu\text{mol/dpm}$ ) and the 0.7–10  $\mu\text{m}$  particulate fraction (an average POC/ $^{234}\text{Th}$  of 37  $\mu\text{mol/dpm}$ ). In other words, POC/ $^{234}\text{Th}$  ratios increased with decreasing particle size.

Surface waters, the Chl-*a* maximum layer, and bottom waters all show a similar  $^{234}\text{Th}$  partitioning pattern in the particulate phase (Table 4 and Figs. 2 and 3). Higher percentages of  $^{234}\text{Th}$  in the 10–53 and the  $>53\ \mu\text{m}$  particle fractions indicate that either the medium and larger particles scavenge  $^{234}\text{Th}$  much more efficiently compared to smaller particles, or that  $^{234}\text{Th}$  is transferred from small particles to medium

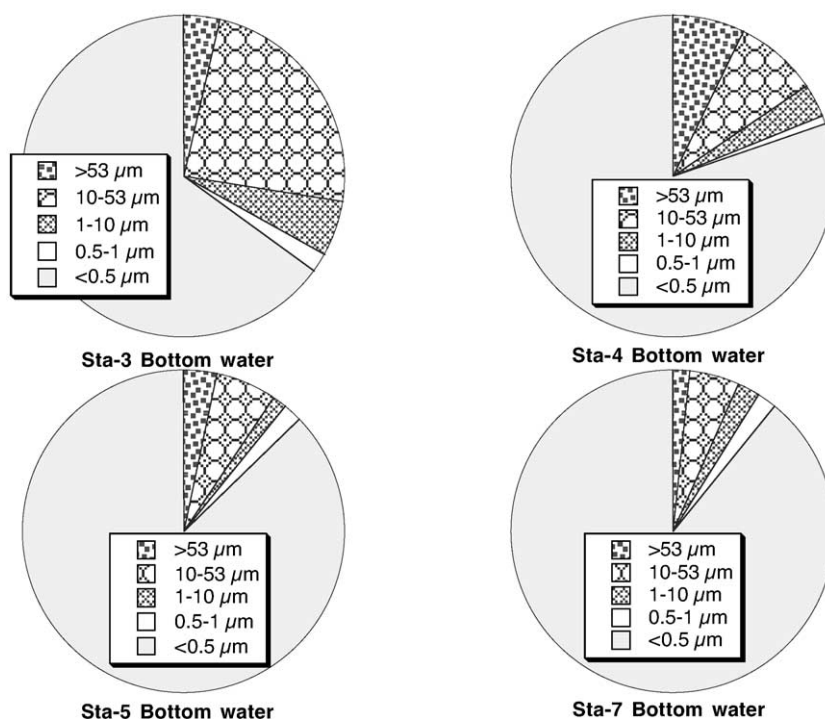


Fig. 3. Partitioning of  $^{234}\text{Th}$  between dissolved and particulate and size-fractionated particles in bottom waters at stations in the Gulf of Mexico.

Table 3  
Concentrations ( $\mu\text{M-C}$ ) of particulate organic carbon (POC) total carbohydrate, uronic acids, and total acid polysaccharides (APS) in size-fractionated particulate fractions

Station	Depth (m)	POC ( $\mu\text{M}$ )			Total carbohydrate ( $\mu\text{M}$ )			Uronic acids ( $\mu\text{M}$ )			Total acid polysaccharides ( $\mu\text{M}$ )		
		0.7–10 $\mu\text{m}$	10–53 $\mu\text{m}$	>53 $\mu\text{m}$	0.7–10 $\mu\text{m}$	10–53 $\mu\text{m}$	>53 $\mu\text{m}$	0.7–10 $\mu\text{m}$	10–53 $\mu\text{m}$	>53 $\mu\text{m}$	0.7–10 $\mu\text{m}$	10–53 $\mu\text{m}$	>53 $\mu\text{m}$
1	2	6.35	0.55	0.42	1.053	0.123	0.035	–	0.0058	0.0023	n.d.	n.d.	n.d.
2	2	4.05	0.17	0.28	0.860	0.052	0.031	0.0256	0.0016	0.0012	0.106	0.0062	0.0009
3	2	4.96	0.19	0.23	0.830	0.077	0.026	0.0193	0.0012	0.0012	0.045	0.0074	0.0008
4	2	4.90	0.075	0.21	0.549	0.027	0.024	0.0165	0.0010	0.0013	0.037	0.0073	0.0005
5	2	2.47	0.26	0.083	0.481	0.053	0.011	0.0198	0.0010	0.0008	0.0535	0.0012	0.0009
5	10	1.98	0.36	0.12	0.344	0.050	0.012	0.0068	0.0018	0.0003	0.0712	0.0012	0.0005
5	30	2.11	0.62	0.11	0.403	0.064	0.017	0.0128	0.0029	0.0003	0.0765	0.0055	0.0005
5	65	2.04	n.d.	0.083	0.353	n.d.	0.017	0.0148	n.d.	0.0003	0.0446	n.d.	0.0004
5	73	2.41	0.49	0.14	0.693	0.069	0.022	0.0144	0.0019	0.0006	0.0627	n.d.	0.0001
6	2	2.03	0.22	0.10	0.361	0.033	0.016	0.0129	0.0008	0.0004	0.0488	0.0037	0.0037
7	1	1.85	n.d.	0.083	0.374	n.d.	0.012	0.0149	n.d.	0.0002	0.0218	n.d.	0.0027
7	10	1.27	n.d.	0.050	0.407	n.d.	0.013	0.0103	n.d.	0.0002	0.0265	n.d.	0.0022
7	35	1.30	n.d.	0.066	0.327	n.d.	0.012	0.0122	n.d.	0.0003	0.0441	n.d.	0.0012
7	45	1.47	n.d.	0.075	0.387	n.d.	0.008	0.0097	n.d.	0.0003	0.0475	n.d.	0.0002
7	75	2.28	n.d.	0.058	0.403	n.d.	0.006	0.0055	n.d.	0.0002	0.0447	n.d.	0.0007

Concentrations of total acid polysaccharides are given in alginic acid equivalents ( $\mu\text{M-C}$ ).

Table 4  
Variations of size-fractionated particulate  $^{234}\text{Th}$  (percent of the total particulate) at surface water, Chl-*a* maximum layer and bottom water

Station	0.5–1 $\mu\text{m}$ (% of total particulate $^{234}\text{Th}$ )	1–10 $\mu\text{m}$ (% of total particulate $^{234}\text{Th}$ )	10–53 $\mu\text{m}$ (% of total particulate $^{234}\text{Th}$ )	>53 $\mu\text{m}$ (% of total particulate $^{234}\text{Th}$ )
<i>Surface water</i>				
5	12.70	17.07	54.45	15.78
6	15.78	15.57	40.28	28.37
7	14.28	17.68	40.56	27.48
<i>Chl-<i>a</i> max layer</i>				
5	11.16	18.09	57.58	13.17
6	12.76	13.26	37.07	36.9
7	8.52	14.94	45.58	30.96
<i>Bottom water</i>				
5	14.63	10.32	48.47	26.58
6	–	–	–	–
7	17.79	21.30	45.20	15.71

and large particles more rapidly than organic carbon is. Since the smaller particles generally have higher specific surface areas and larger particle numbers, the smaller particles should sorb more Th and thus contain higher  $^{234}\text{Th}$  activities (in terms of dpm per unit weight of particles or POC), if surface adsorption would be the only factor controlling the Th scavenging in seawater. However, the opposite is true, i.e.,  $^{234}\text{Th}$ /POC ratios increased with increasing particle size.

As shown in Table 4 and Fig. 2, Th(IV) scavenging and its partitioning between different particulate size fractions does not follow what one would expect from the point of view of direct sorption to different particle size classes of similar chemical composition. However, our observations agree well with coagulation model results, which predict higher  $^{234}\text{Th}$  activity concentrations in the large particles (Burd et al., 2000). Indeed, recent observations indicate that large particles could have lower POC/ $^{234}\text{Th}$  ratios and thus higher OC-specific  $^{234}\text{Th}$  activities (e.g., Buesseler et al., 1995; Bacon et al., 1996; Murray et al., 1996; Guo et al., 1997).

Recent laboratory experiments, using organic matter passing a 0.45- $\mu\text{m}$  filter, have shown that Th(IV) preferentially sorbs to a specific surface-active fibrillar exopolymeric APS of 12.5 kDa molecular weight (Quigley et al., 2002). Marine suspended particles

contain different types of particles and compounds (e.g., Buffle, 1990). It is likely that those surface-active organic components coagulate quickly into larger particles after their production, and, at the same time, strongly interact with particle-reactive Th(IV). This mechanism could be responsible for our observations of large and medium particles having the largest amounts of  $^{234}\text{Th}$  (Figs. 2 and 3) and a decrease of POC/ $^{234}\text{Th}$  ratio with increasing particle size. This had previously been observed by Coale and Bruland (1985), Buesseler et al. (1995), and Murray et al. (1996), and it is consistent with model predictions (Burd et al., 2000). Therefore, Th(IV) appears to follow a more reactive carbon pool and to be transferred much more efficiently from small particles to large particles than organic carbon does (Quigley et al., 2001, 2002), causing higher  $^{234}\text{Th}$  activity in the larger particles. It seems that, in addition to physicochemical sorption, other important factors, such as coagulation and active bacterial and zooplankton activities, which can change the chemical composition of particle surfaces, affect the Th(IV) removal and partitioning in the ocean.

### 3.3. Residence times and fluxes of dissolved, total particulate and size-fractionated particulate $^{234}\text{Th}$ in the water column

According to a simple one-dimensional box model (Bacon and Anderson, 1982; Coale and Bruland, 1985; Buesseler et al., 1992a) and assuming steady state conditions and negligible advective and diffusive transport rates of  $^{234}\text{Th}$ , the residence time ( $\tau$ , days) and flux ( $F_d$  and  $F_p$ , dpm/l/day) of dissolved (d) and particulate (p)  $^{234}\text{Th}$  can be calculated from the following equations:

$$\tau_d = \frac{A_{234}^d}{\lambda_{234}(A_{238} - A_{234}^d)} \quad (3)$$

$$\tau_p = \frac{A_{234}^p}{\lambda_{234}(A_{238} - A_{234}^d - A_{234}^p)} \quad (4)$$

and

$$F_d = \lambda_{234}(A_{238} - A_{234}^d) \quad (5)$$

$$F_p = F_d - A_{234}^p \lambda_{234} = \lambda_{234}(A_{238} - A_{234}^d - A_{234}^p) \quad (6)$$

Where,  $\lambda$  is the decay constant of  $^{234}\text{Th}$  ( $0.0288 \text{ day}^{-1}$ ),  $A_{238}$  is the activity of  $^{238}\text{U}$ , and  $A_{234}^{\text{d}}$  and  $A_{234}^{\text{p}}$  is the activity of dissolved (d) and particulate (p)  $^{234}\text{Th}$ , respectively.

For size-fractionated particulate fractions, we consider a multi-box model with only serial reactions. In other words, Th(IV) is assumed to sorb only onto small particles, which then coagulate from smaller particles into larger particles, without simultaneous (parallel) reactions with all particle size fractions. The predominance of serial over parallel reactions has been verified for  $^{234}\text{Th}$  sorption to marine particles in the laboratory (e.g., Quigley et al., 2001). These authors showed that 90% and more of the particulate  $^{234}\text{Th}$  originated from slower coagulation rather than the rapid initial sorption reaction. Thus, the residence times ( $\tau$ , days) and fluxes ( $F$ , dpm/l/day) of different size fractions of particulate  $^{234}\text{Th}$ , namely, 0.5–1  $\mu\text{m}$  ( $P_1$ ), 1–10  $\mu\text{m}$  ( $P_2$ ), 10–53  $\mu\text{m}$  ( $P_3$ ), and the >53  $\mu\text{m}$  ( $P_4$ ), can be estimated from the following equations:

$$\frac{d\text{Th}_d}{dt} = \lambda_{234}(A_{238} - A_{234}^{\text{d}}) - F_d \quad (7)$$

$$\frac{d\text{Th}_{p1}}{dt} = F_d - \lambda_{234}A_{p1} - F_{p1} \quad (8)$$

$$\frac{d\text{Th}_{p2}}{dt} = F_{p1} - \lambda_{234}A_{p2} - F_{p2} \quad (9)$$

$$\frac{d\text{Th}_{p3}}{dt} = F_{p2} - \lambda_{234}A_{p3} - F_{p3} \quad (10)$$

$$\frac{d\text{Th}_{p4}}{dt} = F_{p3} - \lambda_{234}A_{p4} - F_{p4} \quad (11)$$

where  $F$  is the flux for dissolved (d, <0.5  $\mu\text{m}$ ), 0.5–1  $\mu\text{m}$  ( $P_1$ ), 1–10  $\mu\text{m}$  ( $P_2$ ), 10–53  $\mu\text{m}$  ( $P_3$ ), and the >53  $\mu\text{m}$  ( $P_4$ ) particulate fractions.  $F_{p4}$  is the sinking term for large particles (>53  $\mu\text{m}$ ). Accordingly, the residence time of each particulate fraction can be calculated by:

$$\tau_{p1} = \frac{A_{p1}}{F_{p1}} \quad (12)$$

$$\tau_{p2} = \frac{A_{p2}}{F_{p2}} \quad (13)$$

$$\tau_{p3} = \frac{A_{p3}}{F_{p3}} \quad (14)$$

$$\tau_{p4} = \frac{A_{p4}}{F_{p4}} \quad (15)$$

As shown in Table 5, residence times of dissolved  $^{234}\text{Th}$  ranged from 4–20 days at shallow stations (sta-2 to sta-4) to about 100 days in the upper water column at the deep stations. Residence times of total particulate  $^{234}\text{Th}$  (the >0.5  $\mu\text{m}$  fraction), on the other hand, were much shorter compared to those of dissolved  $^{234}\text{Th}$ , varying from 2–3 days at the shallow stations to 4–20 days in the upper water column of the deep stations (Table 5). According to this serial multi-box model, the residence times for the four different particulate  $^{234}\text{Th}$  size fractions, i.e., the 0.5–1, 1–10, 10–53, and >53  $\mu\text{m}$ , were also significantly shorter than those of dissolved  $^{234}\text{Th}$ . Furthermore, the smaller particulate fractions, both the 0.5–1 and 1–10, and the >53  $\mu\text{m}$  fraction had the shortest residence times, whereas the 10–53  $\mu\text{m}$  particulate fraction had a residence time close to that of the total particulate  $^{234}\text{Th}$ . Short residence times indicate that the smaller particles and the >53  $\mu\text{m}$  particles are turning over in the upper water column on a much shorter time scale. Thus, smaller particles (submicron and micron sized) are the most important intermediary in the scavenging of  $^{234}\text{Th}$  and other trace elements in the ocean, likely due to their high acid polysaccharide concentrations (see later section).

Using data given in Table 2, the dissolved and particulate  $^{234}\text{Th}$  fluxes from the upper 75 or 125 m water column can be estimated. In the upper 75 m water column, the predicted integrated  $^{234}\text{Th}_d$  fluxes ranged from 1334 dpm/m<sup>2</sup>/day at Sta-6 to 2390 dpm/m<sup>2</sup>/day at Sta-5, while the predicted  $^{234}\text{Th}_p$  fluxes varied from 918 dpm/m<sup>2</sup>/day at Sta-7 to 2124 dpm/m<sup>2</sup>/day at Sta-5. Considering the upper 125 m water column, the integrated flux was 2067–3787 dpm/m<sup>2</sup>/day for the dissolved  $^{234}\text{Th}$  and 1416–3148 dpm/m<sup>2</sup>/day for the particulate  $^{234}\text{Th}$  flux. In general, dissolved and particulate  $^{234}\text{Th}$  fluxes were highest at Sta-5 (the CCR station) followed by Sta-7 and Sta-6.

Higher particulate  $^{234}\text{Th}$  fluxes at the CCR station Sta-5 (2124–3148 dpm/m<sup>2</sup>/day) are consistent with

Table 5  
Residence times (days) and fluxes (dpm/l/day) of dissolved, particulate and size fractionated particulate <sup>234</sup>Th

Station	Depth (m)	Salinity	$\tau_{\text{diss}}$ (day)	$\tau_{\text{part}}$ (day)	$\tau_{0.5-1}$ (day)	$\tau_{1-10}$ (day)	$\tau_{10-53}$ (day)	$\tau_{>53}$ (day)	Flux <sub>d</sub> (dpm/l/d)	Flux <sub>p</sub> (dpm/l/d)	Flux <sub>p1</sub> (dpm/l/d)	Flux <sub>p2</sub> (dpm/l/d)	Flux <sub>p3</sub> (dpm/l/d)	Flux <sub>p4</sub> (dpm/l/d)
1	2	35.289	13.7	1.8	0.14	0.23	1.19	0.20	0.0516	0.049	0.051	0.051	0.049	0.049
2	2	35.400	5.9	2.2	0.19	0.63	0.69	0.63	0.0616	0.058	0.061	0.060	0.059	0.058
3	2	35.751	8.4	2.5	0.21	0.53	1.05	0.63	0.0587	0.055	0.058	0.057	0.056	0.055
3	22	35.751	4.0	2.3	0.13	0.35	1.55	0.24	0.0654	0.061	0.065	0.065	0.062	0.061
4	2	36.1	19.9	3.1	0.31	0.25	1.61	0.79	0.0468	0.043	0.046	0.046	0.044	0.043
4	50	36.1	18.1	5.1	0.19	0.75	2.10	1.84	0.0484	0.042	0.048	0.047	0.044	0.042
5	2	36.322	35.9	3.4	0.40	0.54	1.82	0.53	0.0363	0.033	0.036	0.035	0.034	0.033
	2-B	36.322	33.4	7.4	0.76	1.45	2.66	1.97	0.0378	0.031	0.037	0.036	0.033	0.031
	10	36.317	39.6	4.6	0.92	1.04	1.41	1.04	0.0346	0.031	0.034	0.033	0.031	0.031
	30	36.319	46.6	5.1	0.48	1.59	1.99	0.86	0.0317	0.028	0.031	0.030	0.028	0.028
	65	36.409	58.7	4.8	0.64	1.24	1.92	0.76	0.0276	0.024	0.027	0.026	0.025	0.024
	75	36.414	53.9	4.0	0.41	0.67	2.29	0.53	0.0291	0.026	0.029	0.028	0.027	0.026
	300	36.387	80.5	47.6	1.71	4.45	3.88	27.8	0.0224	0.009	0.021	0.019	0.017	0.009
	800	35.832	218	391	5.39	4.28	47.6	106	0.1000	0.001	0.009	0.008	0.003	0.001
6	2	36.556	73.2	8.1	1.07	1.08	3.05	2.29	0.0240	0.019	0.023	0.023	0.021	0.020
	10	36.605	140	10.5	1.37	1.63	4.81	1.79	0.0148	0.011	0.014	0.014	0.012	0.011
	30	36.599	77.5	12.6	1.31	2.69	3.65	3.62	0.0231	0.017	0.022	0.021	0.019	0.017
	40	36.558	109	15.7	1.79	1.92	7.91	2.29	0.0180	0.012	0.017	0.016	0.013	0.012
	74	36.451	248	104	3.68	4.30	18.3	38.5	0.0091	0.002	0.008	0.007	0.005	0.002
	120	36.417	215	28.9	–	–	–	–	0.0103	0.006	–	–	–	–
	500	36.417	311	–	–	–	–	–	0.0073	–	–	–	–	–
	1000	34.920	208	22.6	–	–	–	–	0.0102	0.006	–	–	–	–
	1360	34.971	154	12.1	–	–	–	–	0.0131	0.009	–	–	–	–
7	10	36.672	94.7	16.2	2.27	2.97	6.71	2.22	0.0201	0.014	0.019	0.017	0.015	0.014
	35	36.674	102	10.5	0.85	1.83	5.29	1.66	0.0189	0.014	0.018	0.018	0.015	0.015
	45	36.509	142	19.1	0.66	4.34	8.91	2.63	0.0146	0.009	0.014	0.013	0.010	0.009
	75	36.512	107	20.9	2.62	3.49	8.65	2.91	0.0183	0.011	0.017	0.015	0.012	0.011
	121	36.484	82.8	10.8	0.72	1.30	4.47	3.33	0.0220	0.017	0.022	0.021	0.018	0.017
	202	36.442	144	35.5	2.04	4.31	11.4	9.66	0.0144	0.007	0.014	0.012	0.009	0.007
	500	36.754	160	343	2.19	8.14	69.7	59.8	0.0134	0.001	0.013	0.010	0.003	0.001
	1000	34.909	124	36.1	4.16	3.59	12.4	7.44	0.0155	0.008	0.014	0.013	0.009	0.008
	1500	34.969	89.5	15.9	2.06	2.65	6.69	2.49	0.0199	0.014	0.019	0.018	0.015	0.014

its higher nutrient concentrations and phytoplankton biomass due to upwelling (Table 1). Station 7 is a WCR station, which contained mostly oligotrophic waters and lower Chl-*a* concentrations (Table 1). Therefore, relatively lower particulate  $^{234}\text{Th}$  fluxes at sta-7 (918–1643 dpm/m<sup>2</sup>/day) are in agreement with what one would expect for oligotrophic waters. Station 6 is at the boundary between CCR and WCR, but its particulate  $^{234}\text{Th}$  fluxes (936–1416 dpm/m<sup>2</sup>/day) were very similar to those measured at the WCR station.

### 3.4. Relationship between particulate $^{234}\text{Th}$ and polysaccharide contents

Concentrations of POC, total APS, uronic acids (URA), and total carbohydrates (CHO) in size-fractionated suspended particles are listed in Table 3. These data were used, along with  $^{234}\text{Th}$  data (Table 2), to explore the relationship between  $^{234}\text{Th}$  scavenging and particulate chemical composition. While we found negative or no significant direct relationship between  $^{234}\text{Th}$  activity concentration and POC, CHO,

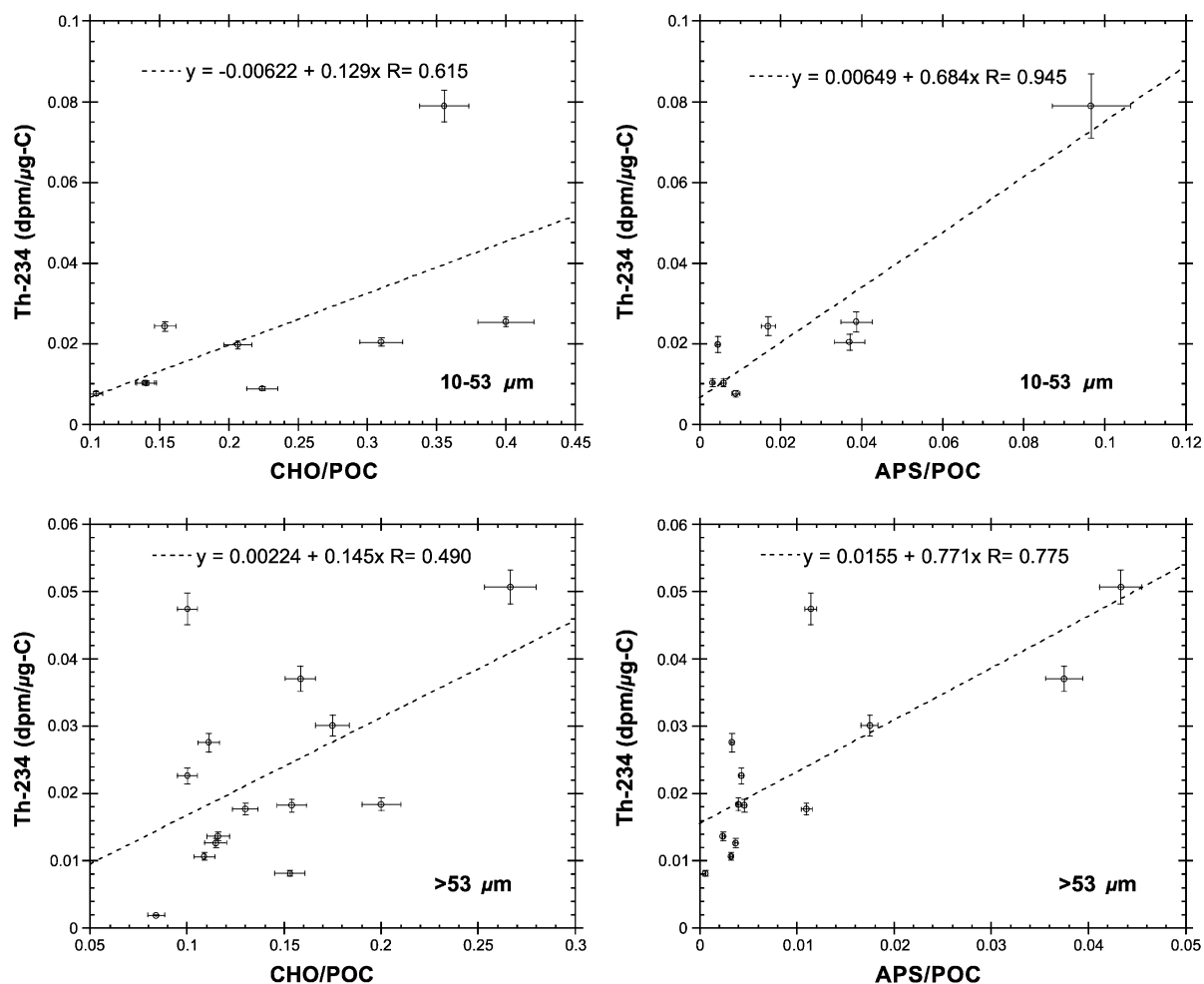


Fig. 4. Relationship between OC-normalized  $^{234}\text{Th}$  and total carbohydrate (CHO) or acid polysaccharide (APS) contents in suspended particles (the >53 and the 10–53 μm fractions). Notice that APS is only a small fraction of the CHO in particles but the correlation coefficients between  $^{234}\text{Th}$  and APS are consistently higher than those between  $^{234}\text{Th}$  and CHO ( $p < 0.005$  vs.  $p < 0.2$  for the 10–53 μm fraction; and  $p < 0.002$  vs.  $p < 0.1$  for the >53 μm fraction).

APS or uronic acid concentrations in size-fractionated suspended particles, linear correlations were greatly improved after normalizing the values of compounds other than POC to organic carbon, which corrects for compositional differences (Fig. 4). For example, OC-normalized  $^{234}\text{Th}$  correlates not only with OC-normalized total CHO ( $R=0.615$  and  $p<0.02$  for the 10–53  $\mu\text{m}$  particles, and  $R=0.49$  and  $p<0.1$  for the  $>53$   $\mu\text{m}$  particles), but also with OC-normalized APS concentrations ( $R=0.945$  and  $p<0.005$  for the 10–53  $\mu\text{m}$  particles and  $R=0.78$  and  $p<0.002$  for the  $>53$   $\mu\text{m}$  particles). Since total carbohydrate (CHO) is usually the largest POC component (e.g., Wang et al., 1996) and total APS is only a minor fraction of CHO (Hung et al., submitted for publication), significantly higher correlation coefficients for the relationship between OC-normalized APS and  $^{234}\text{Th}$  than those between OC-normalized CHO and  $^{234}\text{Th}$  indicate that APS is likely the polysaccharide component controlling the  $^{234}\text{Th}$  uptake in the ocean (Fig. 4).

Even more importantly, residence times of size-fractionated particulate  $^{234}\text{Th}$  are significantly correlated with URA (but weakly correlated with total APS,  $p>0.2$ ) concentrations (Fig. 5), indicating that specific acid polysaccharides (but not all polysaccharides) may control  $^{234}\text{Th}$  scavenging and coagulation rates of particles. In general, residence times of particulate  $^{234}\text{Th}$  decreased with increasing URA concentrations, especially when URA concentrations were lower. When assuming a linear relationship, it is significant ( $R=0.67$  and  $p<0.05$  for the 10–53  $\mu\text{m}$  fraction and  $R=0.64$  and  $p<0.05$  for the  $>53$   $\mu\text{m}$  fraction). Why here uronic acids (a subfraction of total APS), but not total APS, are better predictors of the dynamic behavior of particles and  $^{234}\text{Th}$ , is not clear. It might indicate that not all APS are equally important in  $^{234}\text{Th}$  scavenging, or that the analytical assessment of the surface-active compounds still needs improvements.

Extracellular APS had been previously implicated in trace metal removal (e.g., Croot et al., 2000; Shah et al., 2000), and are among the most surface-reactive compounds in the marine organic carbon pool (Alldredge and Silver, 1988). They also have relatively fast turnover rates in the ocean, as they have modern or younger radiocarbon ages, despite the fact that the bulk organic carbon can be quite old (Santschi et al., 1998). For example. A polysaccharide-enriched

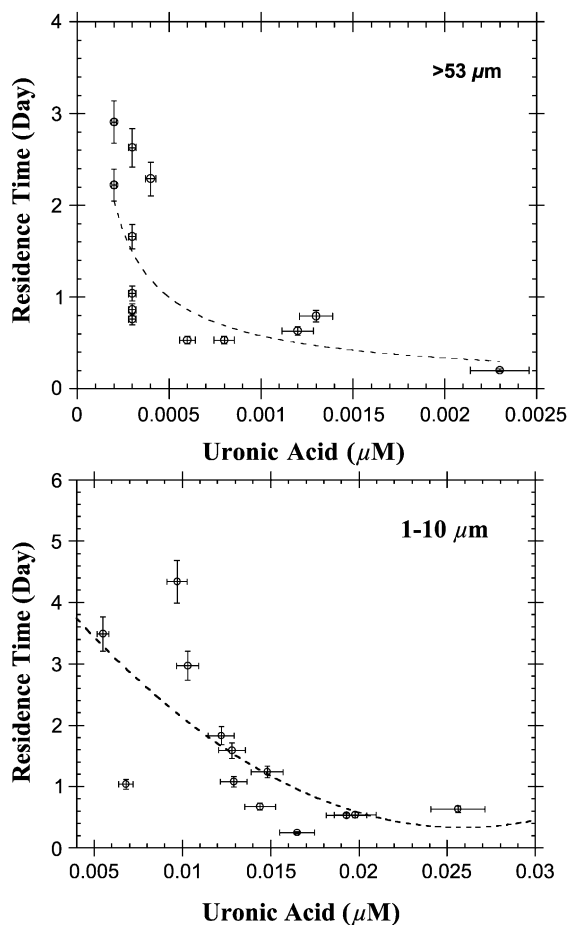


Fig. 5. Relationship between residence times of size-fractionated particulate  $^{234}\text{Th}$  and uronic acid (URA) concentrations in the water column. The linear correlation coefficient is 0.64 ( $p<0.05$ ) for the  $>53$   $\mu\text{m}$  fraction and 0.67 ( $p<0.05$ ) for the 1–10  $\mu\text{m}$  particulate fraction, respectively.

COM sample, with a 98% polysaccharide content, had a  $\Delta^{14}\text{C}$  value of +26‰ vs. –112‰ for the bulk COM (Santschi et al., 1998). Our field study demonstrates a quantitative relation between particle-reactive  $^{234}\text{Th}$  and surface-active exopolymers, further supporting our recent laboratory results on Th(IV) complexation to marine organic compounds, which showed highest affinity of Th(IV) to acid polysaccharides (Quigley et al., 2002). Furthermore, our conclusions about the role of APS in Th(IV) scavenging and coagulation are consistent with the surface-active nature of exopolymeric organic matter widely observed in oceanic environments (e.g., Alldredge

and Silver, 1988; Passow et al., 1994; Mopper et al., 1995).

#### 4. Summary and conclusions

Oceanographically consistent vertical profiles of dissolved and particulate  $^{234}\text{Th}$  concentrations were observed at all three deep stations, with considerable  $^{234}\text{Th}$  deficit relative to  $^{238}\text{U}$  in the upper water column, but reaching a secular equilibrium between  $^{234}\text{Th}$  and  $^{238}\text{U}$  in intermediate waters between 500 and 800 m depth. However, in contrast to Th-profiles in central ocean gyres,  $^{234}\text{Th}/^{238}\text{U}$  disequilibria were observed not only in the upper water column but also in bottom waters at the 1500-m-deep WCR station, likely due to the presence of bottom nepheloid layers, caused by strong boundary currents.

Particulate  $^{234}\text{Th}$  was size fractionated into four size fractions, namely the 0.5–1, 1–10, 10–53, and >53  $\mu\text{m}$  fractions. It was found that the 10–53  $\mu\text{m}$  particulate phase had the largest share of particulate  $^{234}\text{Th}$  (37–57%), followed by the >53  $\mu\text{m}$  (13–36%) and the 1–10  $\mu\text{m}$  (10–21%) and 0.5–1  $\mu\text{m}$  (8–17%) fractions, giving rise to a decrease of POC/ $^{234}\text{Th}$  ratios, or an increase of  $^{234}\text{Th}$ /POC ratios, with increasing particle size, suggesting a control of POC/ $^{234}\text{Th}$  ratio by particulate chemical composition.

Residence times of size-fractionated particulate  $^{234}\text{Th}$ , calculated using a serial multi-box model, were consistently shorter than those for the total particulate  $^{234}\text{Th}$ . Both smaller particles, i.e., 0.5–1 and 1–10  $\mu\text{m}$ , and larger particles, i.e., the >53  $\mu\text{m}$ , had the shortest residence times, ranging from <0.2–1 days at shallow stations to <1–5 days in the upper water column at the deep stations. Short residence times for smaller particles indicates fast coagulation rates, while rapid sinking rates are responsible for the short residence time for the >53  $\mu\text{m}$  particles. Thus, micron-sized and submicron particles are critical intermediaries in the Th(IV) sorption and coagulation process, whereas large (>53  $\mu\text{m}$ ) particles are important in the removal of particulate  $^{234}\text{Th}$  through the sinking pathway.

Particles of a specific size class showed increasing OC-normalized acid polysaccharide, APS, contents with increasing OC-normalized  $^{234}\text{Th}$  activity concentrations and decreasing  $^{234}\text{Th}_p$  residence times. The

surface-active nature of APS makes them the most effective  $^{234}\text{Th}$ -specific scavenging compounds. This is because APS control not only the sorption of  $^{234}\text{Th}$ , but also the coagulation rates of particles in the upper water column. Therefore, the chemical and biological compositions of marine particles (e.g., APS content) play an important role in the scavenging of  $^{234}\text{Th}$  in the ocean and should be considered in Th(IV) scavenging models.

#### Acknowledgements

We wish to thank Chris Noll, Kathy A. Schwehr, Nicolas G. Alvarado-Quiroz, Kent Warnken, Jennifer Haye, Jayne Vidas, and Captain and crew members of the R/V Gyre for their help in sample collection, Kim Roberts, Jayne Vidas and Chris Noll for their technical assistance during sample processing, Jay Pinckney for providing Chl-*a* data, and two anonymous reviewers for constructive comments. This study was supported, in part, by the NSF (OCE-9906823), the Texas Institute of Oceanography, and the Frontier Research System for Global Change/International Arctic Research Center/UAF.

*Associate editor:* Dr. Willard Moore.

#### References

- Allredge, A.L., Silver, M.W., 1988. Characteristics, dynamics and significance of marine snow. *Prog. Oceanogr.* 20, 41–82.
- Bacon, M.P., Anderson, R.F., 1982. Distribution of thorium isotopes between dissolved and particulate forms in the deep sea. *J. Geophys. Res.* 87, 2045–2056.
- Bacon, M.P., Rutgers van der Loeff, M., 1989. Removal of thorium-234 by scavenging in the bottom nepheloid layer of the ocean. *Earth Planet. Sci. Lett.* 92, 157–164.
- Bacon, M.P., Cochran, J.K., Hirschberg, D., Hammar, T.R., Fleer, A.P., 1996. Export flux of carbon at the equator during the EqPac time-series cruises estimated from  $^{234}\text{Th}$  measurements. *Deep-Sea Res.* 43, 1133–1154.
- Baskaran, M., Santschi, P.H., Benoit, G., Honeyman, B.D., 1992. Scavenging of thorium isotopes by colloids in seawater of the Gulf of Mexico. *Geochim. Cosmochim. Acta* 56, 3375–3388.
- Baskaran, M., Murphy, D.J., Santschi, P.H., Orr, J.C., Schink, D.R., 1993. A method for rapid in situ extraction of Th, Pb and Ra isotopes from large volumes of seawater. *Deep-Sea Res.* 40, 849–865.
- Baskaran, M., Santschi, P.H., Guo, L., Bianchi, T.S., Lambert, C., 1996.  $^{234}\text{Th}/^{238}\text{U}$  disequilibria in the Gulf of Mexico: the im-

- portance of organic matter and particle concentration. *Cont. Shelf Res.* 16, 353–380.
- Bruland, K.H., Coale, K.H., 1986. Surface water  $^{234}\text{Th}/^{238}\text{U}$  disequilibria: spatial and temporal variations of scavenging rates within Pacific Ocean. In: Burton, J.D., Brewer, P.G., Chesselet, R. (Eds.), *Dynamic Processes in the Chemistry of the Upper Ocean*. NATO Conf. Ser. Plenum, New York, pp. 159–172.
- Buesseler, K.O., 1998. The decoupling of production and particulate export in the surface ocean. *Global Biogeochem. Cycles* 12, 297–310.
- Buesseler, K.O., Bacon, M.P., Cochran, J.K., Livingston, H.D., 1992a. Carbon and nitrogen export during the JGOFS North Atlantic bloom experiment estimated from  $^{234}\text{Th}/^{238}\text{U}$  disequilibria. *Deep-Sea Res.* 39, 1115–1137.
- Buesseler, K.O., Cochran, J.K., Bacon, M.P., Livingston, H.D., Casso, S.A., Hirschberg, D., Hartman, M.C., Fler, A.P., 1992b. Determination of thorium isotopes in seawater by non-destructive and radiochemical procedures. *Deep-Sea Res.* 39, 1103–1114.
- Buesseler, K.O., Andrews, J.A., Hartman, M.C., Belastock, R., Chai, F., 1995. Regional estimates of the export flux of particulate organic carbon derived from thorium-234 during the JGOFS EQPAC program. *Deep-Sea Res., Part II* 42, 777–804.
- Buffle, J., 1990. *Complexation Reactions in Aquatic Systems: An Analytical Approach*. Ellis Horwood, New York.
- Burd, A.B., Moran, S.B., Jackson, G.A., 2000. A coupled adsorption–aggregation model of the POC/ $^{234}\text{Th}$  ratio of marine particles. *Deep-Sea Res., Part I* 47, 103–120.
- Charette, M.A., Moran, S.B., 1999. Rates of particle scavenging and particulate organic carbon export estimated using  $^{234}\text{Th}$  as a tracer in the subtropical and equatorial Atlantic Ocean. *Deep-Sea Res.* 46, 885–906.
- Coale, K.H., Bruland, K.W., 1985.  $^{234}\text{Th}/^{238}\text{U}$  disequilibria within the California Current. *Limnol. Oceanogr.* 30, 22–33.
- Cochran, J.K., Buesseler, K.O., Bacon, M.P., Livingston, H.D., 1992. Thorium isotopes as indicators of particle dynamics in the upper ocean: results from the JGOFS North Atlantic Bloom Experiment. *Deep-Sea Res.* 40, 1569–1595.
- Cochran, J.K., Barnes, C., Achman, D., Hirschberg, D.T., 1995. Thorium-234/Uranium-238 disequilibrium as an indicator of scavenging rates and particulate organic carbon fluxes in the Northeast Water Polynya, Greenland. *J. Geophys. Res.* 100 (C3), 4399–4410.
- Croot, P.L., Moffett, J.W., Brand, L.E., 2000. Production of extracellular Cu complexing ligands by eucaryotic phytoplankton in response to Cu stress. *Limnol. Oceanogr.* 45, 619–627.
- De Philippis, R., Vincenzini, M., 1998. Exocellular polysaccharides from cyanobacteria and their possible applications. *FEMS Microbiol. Rev.* 22, 151–175.
- Guo, L., Santschi, P.H., 1997. Isotopic and elemental characterization of colloidal organic matter from the Chesapeake Bay and Galveston Bay. *Mar. Chem.* 59, 1–15.
- Guo, L., Santschi, P.H., Baskaran, M., Zindler, A., 1995. Distribution of dissolved and particulate  $^{230}\text{Th}$  and  $^{232}\text{Th}$  in seawater from the Gulf of Mexico and off Cape Hatteras as measured by SIMS. *Earth Planet. Sci. Lett.* 133, 117–128.
- Guo, L., Santschi, P.H., Baskaran, M., 1997. Interaction of thorium isotopes with colloidal organic matter in oceanic environments. *Colloids Surf., A* 120, 255–271.
- Hamilton, P., Lugo-Fernandez, A., 2001. Observations of high speed deep currents in the northern Gulf of Mexico. *Geophys. Res. Lett.* 28, 2867–2870.
- Hedges, J.I., Stern, J.H., 1984. Carbon and nitrogen determinations of carbonate-containing solids. *Limnol. Oceanogr.* 29, 657–663.
- Huh, C.-A., Prah, F.G., 1995. Role of colloids in upper ocean biogeochemistry in the northeast Pacific elucidated from  $^{238}\text{U}/^{234}\text{Th}$  disequilibria. *Limnol. Oceanogr.* 40, 528–532.
- Hung, C.-C., Santschi, P.H., 2000. Spectrophotometric determination of total uronic acids in seawater using cation exchange separation and pre-concentration by lyophilization. *Anal. Chim. Acta* 427, 111–117.
- Hung, C.-C., Tang, D., Warnken, K.W., Santschi, P.H., 2001. Distributions of carbohydrates, including uronic acids, in estuarine waters of Galveston Bay. *Mar. Chem.* 73, 305–318.
- Hung, C.-C., Guo, L., Santschi, P.H., Pinckney, J., Lumsden, E., 2002. Production and distribution of total carbohydrate and acid polysaccharides in the Gulf of Mexico. *Mar. Ecol. Prog. Ser.*, submitted for publication.
- Ku, T.L., Knauss, K.G., Matthew, G.G., 1977. Uranium in the open ocean: concentration and isotopic composition. *Deep-Sea Res.* 24, 1005–1017.
- Mopper, K., Zhou, J., Ramana, K.S., Passow, U., Dam, H.G., Drapreau, D.T., 1995. The role of surface-active carbohydrates in the flocculation of a diatom bloom in a mesocosm. *Deep-Sea Res.* 42, 47–73.
- Moran, S.B., Buesseler, K.O., 1993. Size fractionated  $^{234}\text{Th}$  in continental shelf waters off New England: implications for the role of colloids in oceanic trace metal scavenging. *J. Mar. Res.* 51, 893–922.
- Moran, S.B., Smith, J.N., 2000.  $^{234}\text{Th}$  as a tracer of scavenging and particle export in the Beaufort Sea. *Cont. Shelf Res.* 20, 153–167.
- Murray, J.W., Downs, J.N., Strom, S., Wei, C.L., Jannasch, H.W., 1989. Nutrient assimilation, export production and  $^{234}\text{Th}$  scavenging in the eastern equatorial Pacific. *Deep-Sea Res.* 36, 1471–1489.
- Murray, J.W., Young, J., Newton, J., Dunne, J., Chapin, T., Paul, B., 1996. Export flux of particulate organic carbon from the central Equatorial Pacific determined using a combined drifting trap— $^{234}\text{Th}$  approach. *Deep-Sea Res.* 43, 1095–1132.
- Niven, S.E.H., Keplay, P.E., Budgen, J.B.C., 1997. The role of TEP in  $^{234}\text{Th}$  scavenging during a coastal diatom bloom. In: Germain, P., et al. (Eds.), *Radionuclides in the Oceans RADOCC 96–97 Proceedings, Part I, Cherbourg-Octeville (France)*, pp. 213–218.
- Passow, U., Logan, B.E., Alldredge, A.L., 1994. The role of particulate carbohydrate exudates in the flocculation of diatom blooms. *Deep-Sea Res., Part I* 41, 335–357.
- Quigley, M.S., Honeyman, B.D., Santschi, P.H., 1996. Thorium sorption in the marine environment: equilibrium partitioning at the Hematite/water interface, sorption/desorption kinetics and particle tracing. *Aquat. Geochem.* 1, 277–301.
- Quigley, M.S., Santschi, P.H., Guo, L., Honeyman, B.D., 2001.

- Sorption irreversibility and coagulation behavior of  $^{234}\text{Th}$  with marine organic matter. *Mar. Chem.* 76, 27–45.
- Quigley, M.S., Santschi, P.H., Hung, C.-C., Guo, L., Honeyman, B.D., 2002. Importance of acid polysaccharides for  $^{234}\text{Th}$  complexation to marine organic matter. *Limnol. Oceanogr.* 47, 367–377.
- Santschi, P.H., Honeyman, B.D., 1991. Are thorium scavenging and particle fluxes in the ocean regulated by coagulation? In: Kershaw, P.J., Woodhead, D.S. (Eds.), *Radionuclides in the Study of Marine Processes*. Elsevier, New York, NY, pp. 107–115.
- Santschi, P.H., Guo, L., Baskaran, M., Trumbore, S., Southon, J., Bianchi, T., Honeyman, B., Cifuentes, L.A., 1995. Isotopic evidence for the contemporary origin of high-molecular weight organic matter in oceanic environments. *Geochim. Cosmochim. Acta* 59, 625–631.
- Santschi, P.H., Balnois, E., Wilkinson, K., Zhang, J., Buffle, J., Guo, L., 1998. Fibrillar polysaccharides in marine macromolecular organic matter, as imaged by Atomic Force Microscopy and Transmission Electron Microscopy. *Limnol. Oceanogr.* 43, 896–908.
- Santschi, P.H., Guo, L., Quigley, M.S., Baskaran, M., Walsh, I., 1999. Boundary exchange and scavenging of radionuclides in continental margin waters of the Middle Atlantic Bight: implications for organic carbon fluxes. *Cont. Shelf Res.* 19, 609–636.
- Shah, V., Ray, A., Garg, N., Madamwar, D., 2000. Characterization of the extracellular polysaccharide produced by a marine cyanobacterium, *cyanosphaera* sp. ATCC 51142, and its exploitation toward metal removal from solutions. *Curr. Microbiol.* 40, 274–278.
- Wang, X.C., Druffel, E.R.M., Lee, C., 1996. Radiocarbon in organic compound classes in particulate organic matter and sediment in the deep northeast Pacific Ocean. *Geophys. Res. Lett.* 23, 3583–3586.